IRAM Memo 2015-2

NOEMA sensitivity estimator

J. Pety[1,2], J. Boissier[1], E. Reynier[1], S. Bardeau[1]

1. IRAM (Grenoble)
2. Observatoire de Paris

June, 18^{th} 2024
Version 5.0

Abstract

This memo describes the equations used in the NOEMA sensitivity estimator available in the online sensitivity estimator (`https://oms.iram.fr/tse/#noema`), to be used for proposal preparation and in the `GILDAS/ASTRO` program (so-called detailed estimator, independent of NOEMA call for proposals).

Contents

1 The interferometric point source sensitivity from first principles

1.1 System temperature

The system temperature is a summary of the noise added by the system. This noise comes from 1) the receiver and the optics, 2) the emission of the sky, and 3) the emission picked up by the secondary side lobes of the telescope. It is usual to approximate it (in the $T_{\rm a}^{\star}$ scale) with

$$T_{\rm sys} = \frac{(1+G_{\rm im})\exp\{\tau_{\rm s}\,A\}}{F_{\rm eff}}\left[F_{\rm eff}\,T_{\rm atm}\,(1-\exp\{-\tau_{\rm s}\,A\}) + (1-F_{\rm eff})\,T_{\rm cab} + T_{\rm rec}\right], \tag{1}$$

where $G_{\rm im}$ is the receiver image gain, $F_{\rm eff}$ the telescope forward efficiency, $A = 1/\sin(\text{elevation})$ the airmass, $\tau_{\rm s}$ the atmospheric opacity in the signal band, $T_{\rm atm}$ the mean physical atmospheric temperature, $T_{\rm cab}$ the ambient temperature in the receiver cabine and $T_{\rm rec}$ the noise equivalent temperature of the receiver and the optics. All those parameters are easily measured, except $\tau_{\rm s}$, which depends on the amount of water vapor in the atmosphere and which is estimated by complex atmospheric models.

The $T_{\rm sys}$ value is expressed so that all these terms are corrected for the attenuation by the atmosphere, the coupling of the antenna to the sky, and the side-band rejection. In other words, the system temperature is given in units that assume a perfect antenna (coupling equal to 1) located outside the atmosphere for a single-sideband signal.

1.2 Power and sensitivity measured at the correlator output for one baseline

After the atmopheric calibration that converts the measurement scale from the correlator output (in counts) to the $T_{\rm a}^{\star}$ scale, the output of the correlator for one correlation is a power equivalent temperature (in the Rayleigh-Jeans domain), which is sampled at a rate of $2d\nu$, where $d\nu$ is the frequency bandwidth over which the power is measured. As explained in the previous section, the standard deviation of each power measurement is given by the system temperature power ($T_{\rm sys}$). During the integration time (Δt), $2d\nu\,\Delta t$ independent samples of the signal power are measured to ensure the Nyquist sampling of the signal in the bandwidth $d\nu$. The signal power is averaged over these independent samples. The uncertainty on the averaged signal power, named sensitivity ($\sigma_{\rm K}$), is thus standard deviation of the average or

$$\sigma_{\rm K} = \frac{T_{\rm sys}}{\sqrt{2\,d\nu\,\Delta t}}. \tag{2}$$

1.3 Quantization efficiency

The Analog-to-Digical-Converter (ADC) will quantize the analog signal on a finite number of bits. This can be seen as an additional source of noise that is modeled as a spectrometer efficiency ($\eta_{\rm spec}$) and Eq. 2 becomes

$$\sigma_{\rm K} = \frac{T_{\rm sys}}{\eta_{\rm spec}\sqrt{2\,d\nu\,\Delta t}}. \tag{3}$$

1.4 Collecting the measurements from all baselines

Assuming that the atmosphere and receiving system is independent of the pairs of antenna considered, the previous equation is valid for any baseline of the interferometer. All the visibilities can be averaged into a single visibility to define the point source signal. This implies that the standard deviation (sensitivity) on the point source signal will be divided by the square root of the number of baselines, i.e., the number of pairs of antennas, $n_{\rm ant}\,(n_{\rm ant}-1)/2$, where $n_{\rm ant}$ is the number of antennas. The point source sensitivity is then

$$\sigma_{\rm K} = \frac{T_{\rm sys}}{\eta_{\rm spec}\sqrt{n_{\rm ant}\,(n_{\rm ant}-1)\,d\nu\,\Delta t}}. \tag{4}$$

1.5 From the temperature power to the flux

For a point source, it is more natural to express the signal, and thus the sensitivity, in unit of flux. The flux (F) of a point source is linked to its brightness temperature T through

$$F = J^{\rm sd}_{\rm ant} T \quad \text{with} \quad J^{\rm sd}_{\rm ant} = \frac{2k}{A_{\rm eff}}, \tag{5}$$

where k is the Boltzman constant, and $A_{\rm eff}$ is the effective area of the antenna (eq. 3-113 in Kraus , 1982), and $J^{\rm sd}_{\rm ant}$ the conversion factor for a typical interferometer antenna. The effective area depends on the observing wavelength when the surface rms accuracy becomes a significant fraction of the wavelength. For NOEMA, the effective area is close to 1 at 3 mm but significantly lower than 1 at 1 mm.

Using the same conversion factor for the sensitivity, we yield

$$\sigma_{\rm Jy} = \frac{J^{\rm sd}_{\rm ant}\, T_{\rm sys}}{\eta_{\rm spec}\sqrt{n_{\rm ant}\,(n_{\rm ant}-1)\,d\nu\,\Delta t}}. \tag{6}$$

1.6 Signal decorrelation

$J^{\rm sd}_{\rm ant}$ characterizes the antenna hardware, *i.e.* it assumes perfect atmospheric conditions or the use of autocorrelations, as in single-dish measurements. In interferometric mode, the phase of the turbulent atmosphere above each antenna of a given baseline has a random part that causes an additional "attenuation" of the amplitude of the correlation. A point source of 1 Jy flux will appear as a source of $\eta_{\rm atm}$ Jy flux if we only use the $J^{\rm sd}_{\rm ant}$ factor. This is called atmospheric decorrelation and it depends on the weather during the observations.

However, the last calibration step of interferometric data is to measure a point source of known flux to deduce the actual conversion factor, $J^{\rm int}_{\rm ant}$, taking into account the atmospheric decorrelation that happens during the observations. By definition of $\eta_{\rm atm}$, we yield

$$J^{\rm sd}_{\rm ant} = \eta_{\rm atm}\, J^{\rm int}_{\rm ant}. \tag{7}$$

It can be shown that $\eta_{\rm atm}$ is related to the atmospheric rms phase noise ($\phi_{\rm rms}$) through

$$\eta_{\rm atm} = e^{-\frac{\phi^2_{\rm rms}}{2}}. \tag{8}$$

1.7 Noise vs signal

One subtlety is that the noise is unaffected by the atmospheric decorrelation, in contrast with the signal, because noise is a random process as the turbulence phase noise.

But the conversion factor, $J^{\rm int}_{\rm ant}$, is applied to the data that can contain signal as well as noise. Any attempt to measure the noise rms on visibilities or imaged data will thus results in a standard deviation larger than the one given in Eq. 6 by a factor $\eta_{\rm atm}$. So when we estimate the noise level of an interferometer, we need to take into account the interferometric conversion factor that depends on the typical weather conditions (i.e., the atmospheric rms phase noise). This gives

$$\sigma_{\rm Jy} = \frac{J^{\rm int}_{\rm ant}\, T_{\rm sys}}{\eta_{\rm spec}\sqrt{n_{\rm ant}\,(n_{\rm ant}-1)\,d\nu\,\Delta t}}. \tag{9}$$

2 The interferometric extended source sensitivity

2.1 Starting from the point source sensitivity

As a summary, the point source sensitivity for an interferometric measurement reads

$$\sigma_{\rm Jy} = \frac{J^{\rm int}_{\rm ant}\, T_{\rm sys}}{\eta_{\rm spec}\sqrt{n_{\rm ant}\,(n_{\rm ant}-1)\,d\nu\,\Delta t}}, \tag{10}$$

where $\sigma_{\rm Jy}$ is the rms noise flux obtained by integration with an interferometer of $n_{\rm ant}$ identical antenna during the Δt integration time in a frequency resolution $d\nu$ with a system temperature given by $T_{\rm sys}$. $J^{\rm int}_{\rm ant}$ is the conversion factor of a typical interferometer antenna taking into account the typical amount of atmospheric decorrelation at the observed wavelength.

Equation 10 is true only when the source is unresolved, *i.e.*, there is no effect of beam dilution. In practice this is rarely the case because the interferometer tries to resolve the source. Thus, this noise formula should be used with caution when preparing the observations. In practice, this formula is useful when one wishes to compare the sensitivity of two different interferometer. Indeed, this point source sensitivity is independent of the interferometer synthesized beam that depends on the details of the observations and, in particular, the interferometer configuration and the completeness of the Earth synthesis.

2.2 We yield the interferometric extended source sensitivity

The point source sensitivity is well adapted to unresolved sources because it directly delivers the estimation of the flux of these sources. For extended sources, the point source sensitivity is expressed in unit of Jy/Beam that is difficult to understand because it depends on the synthesized beam resolution in a non-trivial way. When a source is resolved (extended compared to the expected synthesized beam), it is much easier to think in temperature brightness. We thus convert back to a brightness temperature scale, but we now do it at the synthesized beam resolution.

After calibration (including the calibration of the atmospheric decorrelation), imaging, and deconvolution (including a potential phase self-calibration), an interferometer mimick the observation by a telescope of angular resolution equal to the synthesized beam. However, the notion of effective collecting surface is ambiguous in this case. In order to generalize Eq. 5 to the final product of an interferometer, we use the fact that the solid angle resolution (Ω) of a telescope of effective collecting surface $A_{\rm eff}$ is by definition linked to the observing wavelength (λ) through

$$\Omega\, A_{\rm eff} = \lambda^2. \tag{11}$$

We can thus generalize Eq. 5 as

$$F = J_{\rm ant} T \quad \text{with} \quad J_{\rm ant} = \frac{2k\,\Omega}{\lambda^2}. \tag{12}$$

On one hand, we have to use the solid angle of the primary beam $\Omega_{\rm prim}$ for $J^{\rm sd}_{\rm ant}$ and $J^{\rm int}_{\rm ant}$. This yields

$$J^{\rm int}_{\rm ant} = \frac{J^{\rm sd}_{\rm ant}}{\eta_{\rm atm}} = \frac{2k\,\Omega_{\rm prim}}{\eta_{\rm atm}\,\lambda^2}. \tag{13}$$

On the other hand, we have to use the solid angle of the synthesized beam $\Omega_{\rm syn}$ for the conversion factor that we have to apply to the deconvolved product ($J^{\rm syn}_{\rm ant}$)

$$J^{\rm syn}_{\rm ant} = \frac{2k\,\Omega_{\rm syn}}{\lambda^2}. \tag{14}$$

Note that we don't use the decorrelation efficiency in the later equation. This is due to the fact that after the data reduction, the deconvolved product should appear as if it was observed by a perfect antenna whose response is exactly a Gaussian of angular size $\Omega_{\rm syn}$.

Combining Eq. 10, 13, and 14, we yield

$$\sigma_{\rm K} = \frac{\Omega_{\rm prim}}{\Omega_{\rm syn}}\,\frac{1}{\eta_{\rm atm}}\,\frac{T_{\rm sys}}{\eta_{\rm spec}\sqrt{n_{\rm ant}\,(n_{\rm ant}-1)\,d\nu\,\Delta t}}, = \frac{\theta^2_{\rm prim}}{\theta_{\rm maj}\,\theta_{\rm min}}\,\frac{1}{\eta_{\rm atm}}\,\frac{T_{\rm sys}}{\eta_{\rm spec}\sqrt{n_{\rm ant}\,(n_{\rm ant}-1)\,d\nu\,\Delta t}}, \tag{15}$$

where $\sigma_{\rm K}$ is the rms noise brightness, $\theta_{\rm prim}$ the half primary beam width, and $\theta_{\rm maj}$ and $\theta_{\rm min}$ the half beamwidth along the major and minor axes of the synthesized beam.

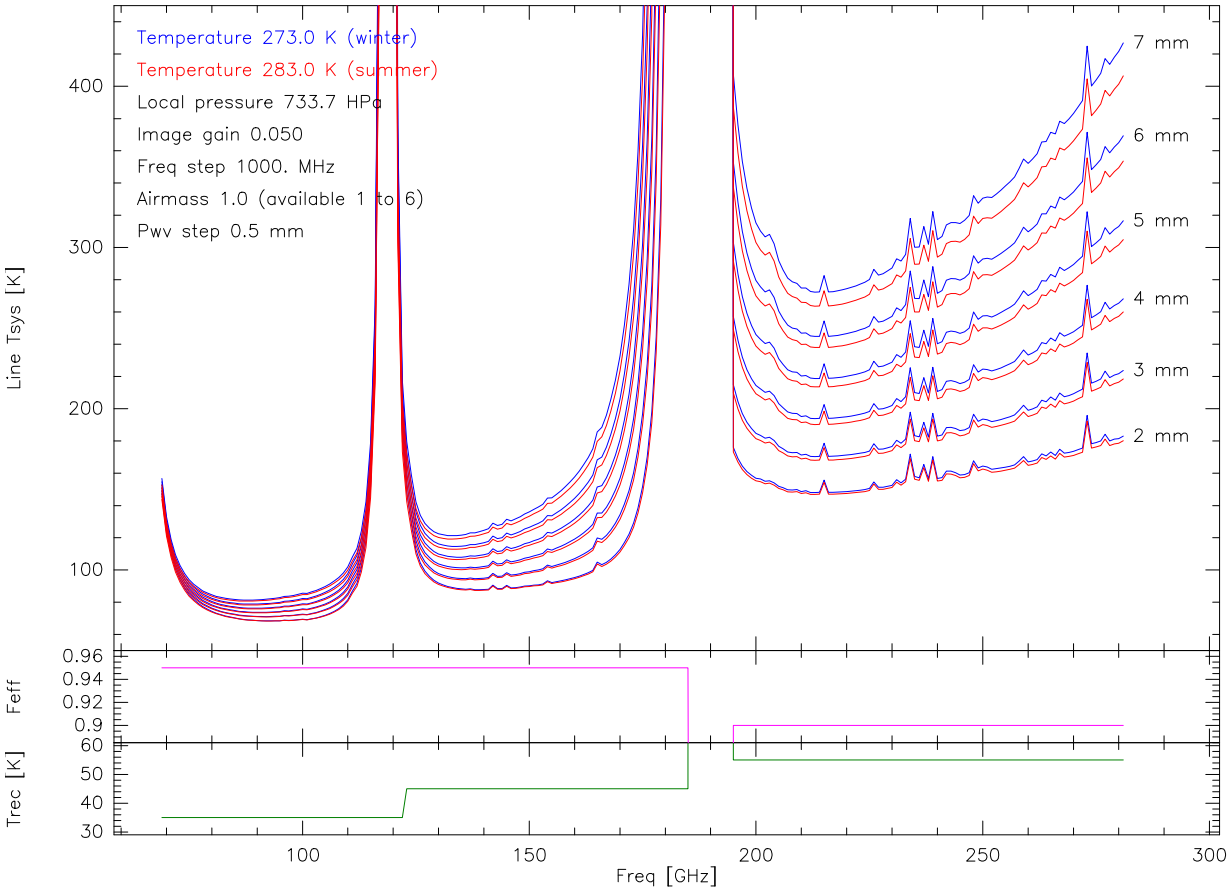

Figure 1: **Top:** Summer (red) and Winter (blue) semester $T_{\rm sys}$ for different precipitable water vapor (PWV) amount and for a source at zenith. The numbers indicate PWV values assumed in the computation. **Middle:** Assumed forward effiencies in the computation. **Bottom:** Assumed receiver temperatures in the computation.

2.3 Interpretation

Equation 15 clearly states that the sensitivity to extended sources depends on the dilution of the synthesized beam in the primary beam. This is why this formulation of the sensitivity is well adapted to resolved sources.

For a given interferometer, the primary beamwidth is a fixed quantity while the synthesized beam is to first order proportional to the longest baseline in the current interferometer configuration. Hence, doubling the largest baseline will multiply $\sigma_{\rm K}$ by a factor $4(=2^2)$ for the same integration time or it will multiply the integration time by a factor $16(=2^4)$ in order to reach the same sensitivity. This just reflects that while the interferometer tries to mimic a single-dish antenna of same diameter as the largest baseline, all the antenna of the interferometer only fill a fraction of the total collecting area of the single-dish, this fractions decreasing with a power of two as the baseline linearly increases.

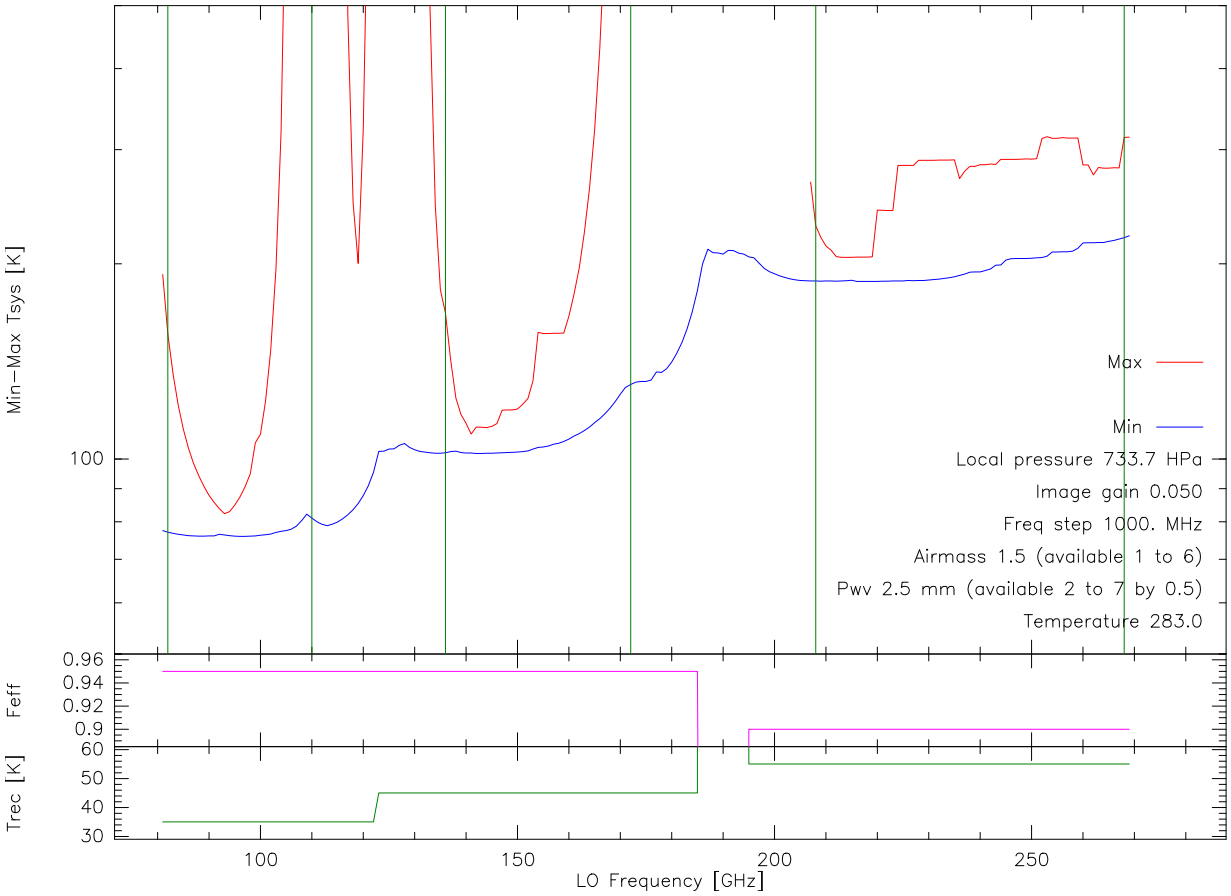

Figure 2: **Top:** Minimum and maximum $T_{\rm sys}$ obtained in the intermediate frequency bandwidth as a function of the local oscillator frequency used in the tuning. **Middle:** Assumed forward effiencies in the computation. **Bottom:** Assumed receiver temperatures in the computation.

3 In practice

3.1 Line vs continuum system temperature

In the online estimator (to be used for proposal preparation), the $T_{\rm sys}$ is interpolated in frequency and airmass from tabulated values (see Fig. 1). The airmass is estimated using the maximum elevation of a source at the chosen Declination. The values are different for summer and winter due to the different atmospheric characteristics. Moreover, the chosen amount of precipitable water vapor depends on the receiver band (in addition to the season) because the NOEMA operation team schedule the different receiver bands according to the actual weather (high frequency bands are scheduled only during the best weather conditions).

In the ASTRO detailed sensitivity estimator, the system temperature is computed using an atmospheric model (ASTRO\ATMOSPHERE command) with ambient temperature and precipitable water amount as input.

The $T_{\rm sys}$ can vary significantly over the large bandwitdh of the 2SB NOEMA receivers. Figure 2 shows the minimum and maximum system temperature inside the IF bandwidth for all possible local oscillator tunings. As a result, for continuum estimation, a frequency averaged $T_{\rm sys}$ is interpolated from a pre-computed table. The relevant frequency in that case is the LO frequency of the tuning (see Fig. 3). The averaging is done such as $1/ < T_{\rm sys} >^2 = 1/N \sum 1/T_{\rm sys}^2$.

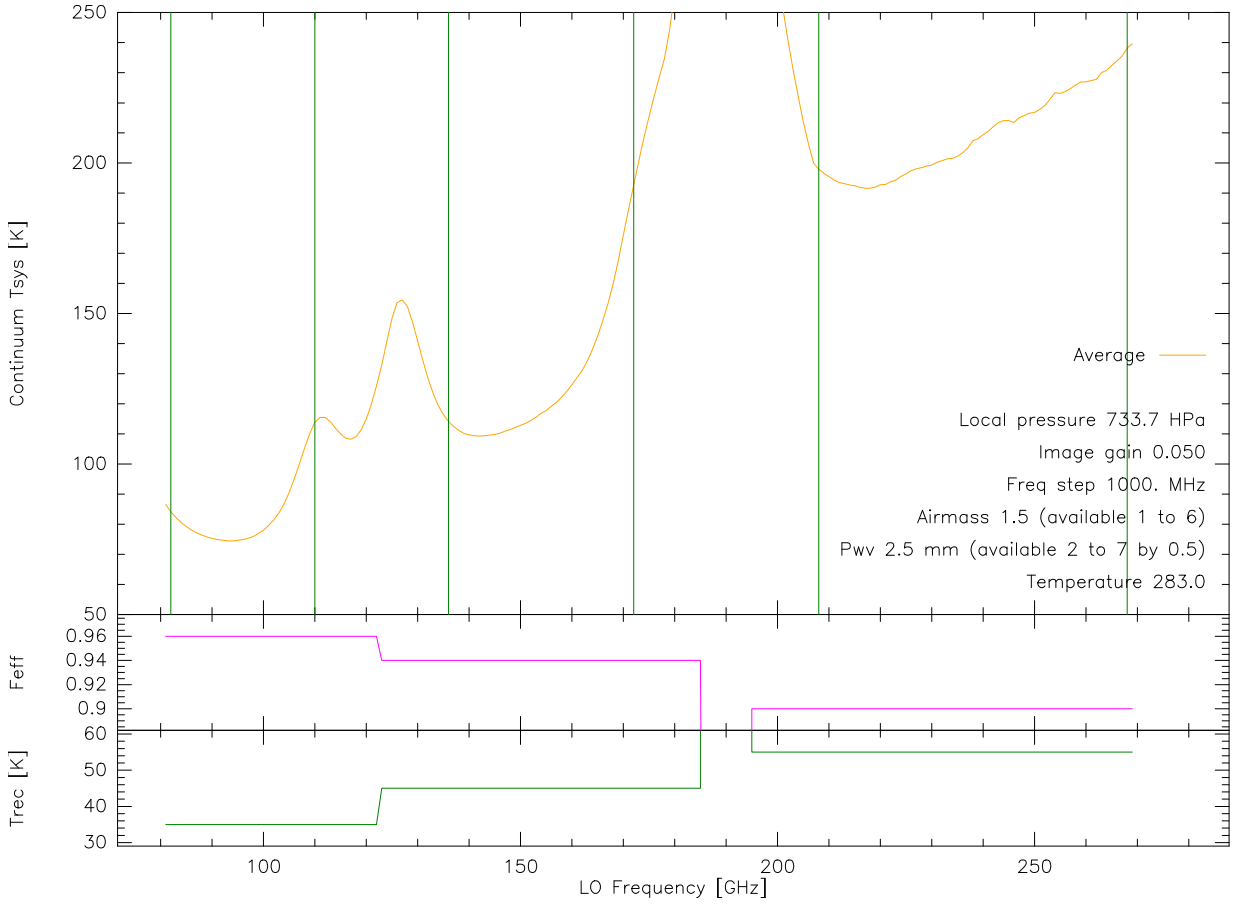

Figure 3: **Top:** Averaged "continuum" $T_{\rm sys}$ as a function of the local oscillator frequency used in the tuning. **Middle:** Assumed forward effiencies in the computation. **Bottom:** Assumed receiver temperatures in the computation.

This is not implemented in the ASTRO detailed estimator, due to the prohibitive computing cost of the atmospheric model over the $2 \times 8\,\mathrm{GHz}$.

3.2 The number of polarizations

All NOEMA antennas are equipped with dual polarization receivers. They measure the signal coming from the pointed direction in two perpendicular polarizations in the same frequency range. For the current generation of receiver (2006) and correlators, one or two polarizations are processed by the correlators, depending on the project settings. We thus have to introduce the number of polarizations $n_{\rm pol}$, which can be set to 1 or 2 and insert it in the radiometer equation with

$$\sigma_{\rm Jy} = \frac{J^{\rm int}_{\rm ant}\, T_{\rm sys}}{\eta_{\rm spec}\sqrt{n_{\rm ant}\,(n_{\rm ant}-1)\,d\nu\,n_{\rm pol}\,\Delta t_{\rm on}}}. \tag{16}$$

3.3 Actual computations

The sensitivity estimator computes the relationship between Δt and $\sigma_{\rm Jy}$ with

$$\sigma_{\rm Jy} = \frac{J^{\rm int}_{\rm ant}\, T_{\rm sys}}{\eta_{\rm spec}\sqrt{n_{\rm ant}\,(n_{\rm ant}-1)\,d\nu\,n_{\rm pol}\,\Delta t_{\rm on}}}, \tag{17}$$

where $T_{\rm sys}$ is interpolated in frequency and airmass from the table, and the other parameters are defined by the observatory. It then computes the relationship between $\sigma_{\rm K}$ and $\sigma_{\rm Jy}$ with

$$\sigma_{\rm K} = \frac{\sigma_{\rm Jy}}{J_{\rm ant}^{\rm syn}} \quad \text{with} \quad J_{\rm ant}^{\rm syn} = \frac{2\pi\, k\, \theta_{\rm maj}\theta_{\rm min}}{4\, \ln 2\, \lambda^2}. \tag{18}$$

4 Observing mode and elapsed telescope time

The goal of a time estimator is to find the elapsed telescope time ($\Delta t_{\rm tel}$) needed to obtain a given rms noise, while a sensitivity estimator aims at finding the rms noise obtained when observing during $\Delta t_{\rm tel}$. The total integration time spent on-source $\Delta t_{\rm on}$ is shorter than the elapsed telescope time due to several factors. As of Gildas Jul17 release, the input time of the sensitivity estimator is telescope time. The actual on source time is then computed taking into account the following two points:

1. **Instrumental setup time:** At the beginning of an observing track a significant time ($\Delta t_{\rm tune} \sim 40$ minutes according to history of observations) is spent in receiver tuning and calibration observations before observing the actual astronomical target. This means that even for a very short ON source time, a project cannot be shorter than $\Delta t_{\rm tune}$. Also, for long projects observed in several ($n_{\rm track}$) tracks the time spent for tuning and calibration is $n_{\rm track} \times \Delta t_{\rm tune}$. We thus define the time spent for observations (i.e. without instrumental setup) $\Delta t_{\rm obs}$ as:

$$\Delta t_{\rm obs} = \Delta t_{\rm tel} - n_{\rm track} \times \Delta t_{\rm tune} \tag{19}$$

   The number of tracks is computed as $n_{\rm track} = \frac{\Delta t_{\rm tel}}{\Delta t_{\rm track}+\Delta t_{\rm tune}}$ where $\Delta t_{\rm track}$ is the typical duration of a track, which depends on the source declination:

   - Sources above 0 deg are observed 8 hours at most,
   - 8.2 hours for a declination of 0 deg (truncated to 8 hours),
   - 6.5 hours for a declination of -10 deg,
   - 3.9 hours for a declination of -20 deg,
   - 0.0 hours for a declination of -30 deg.
   - Sources below -30 deg can not be observed.

   A linear interpolation with the declination is performed in the appropriate range between -30 deg and 0 deg.
   For short projects ($\Delta t_{\rm tel} < \Delta t_{\rm track} + \Delta t_{\rm tune}$), the number of tracks $n_{\rm track}$ is set to 1. Otherwise, the floating value of $n_{\rm track}$ is used in the computation of $\Delta t_{\rm obs}$. Since $\Delta t_{\rm tune}$ is constant whatever the length of a track the use of a floating value for $n_{\rm track}$ is somehow unnatural but it ensures that the conversion from $\Delta t_{\rm tel}$ to $\Delta t_{\rm obs}$ is a monotonic function.

2. **Observing efficiency:** After the initial phase of instrumental setup, the observing mode does not dedicate 100% of the time to the astronomical target. Part of the time is spent for calibration (pointing, focus, atmospheric calibration,...) and to slew the telescopes between useful integrations. The time actually spent on source $\Delta t_{\rm on}$ is defined as

$$\Delta t_{\rm on} = \Delta t_{\rm obs} \times \eta_{\rm tel} \tag{20}$$

   where $\eta_{\rm tel}$ is the observing efficiency.

The exact computation depends on the observing mode. There are three main observation kinds that are exclusive from each other.

Single-source, single-field observations where the telescope tracks a single source during the full integration time. This mode is used when the signal-to-noise ratio is the limiting factor.

Track-sharing, single-field observations where the telescope regularly cycles between a few close-by sources. This mode is used when the sources are so bright that the limiting factor is the Earth synthesis, not the signal-to-noise ratio.

Single-source mosaicking where the telescope regularly cycles between close-by pointings that usually follows a hexagonal compact pattern whose side is $\lambda/(2d_{\rm prim})$, where $d_{\rm prim}$ is the diameter of the interferometer antennas. This modes is used to image sources wider than the primary beam field of view.

These kinds can be combined with two others possibilities.

Dual band observations where the use of an additional dichroic allows the interferometer to observe simultaneously at 3 and 1 mm.

Frequency cycling observations where the tuning frequency is regularly cycled between several predefined values in order to, e.g., allow to observe a full atmospheric window in a single track.

These two additional possibilities can in principle be combined during the same observation.

In the following, we will work out the equations needed by the sensitivity estimator for each of these observing modes.

4.1 Single-source, single-field observations

That's the simplest case. The point source sensitivity in this case is

$$\sigma_{\rm Jy} = \frac{J_{\rm ant}^{\rm int}\, T_{\rm sys}}{\eta_{\rm spec}\sqrt{n_{\rm ant}\,(n_{\rm ant}-1)\,d\nu\,n_{\rm pol}\,\Delta t_{\rm on}}} \tag{21}$$

where $\Delta t_{\rm on}$ is the time spent on-source. It is related to the total elapsed telescope time $\Delta t_{\rm tel}$ through:

$$\Delta t_{\rm on} = \frac{\Delta t_{\rm tel} \;-\; n_{\rm track} \times \Delta t_{\rm tune}}{\eta_{\rm tel}} \tag{22}$$

For single source projects, $\eta_{\rm tel}$ is estimated to be about 1.6. Note that the exact value will depend on several parameters such as the number of calibrators and the distance between the source and the calibrator(s).

4.2 Track-sharing, single-field observations

In this case, the telescope time is equally divided between the $n_{\rm sou}$ observed sources. This yields

$$\sigma_{\rm Jy} = \frac{J_{\rm ant}^{\rm int}\, T_{\rm sys}}{\eta_{\rm spec}\sqrt{n_{\rm ant}\,(n_{\rm ant}-1)\,d\nu\,n_{\rm pol}\,\Delta t_{\rm on}}} \tag{23}$$

$$\text{with}\quad \Delta t_{\rm on} = \frac{\Delta t_{\rm tel} \;-\; n_{\rm track} \times \Delta t_{\rm tune}}{\eta_{\rm tel} \times n_{\rm sou}} \tag{24}$$

Note that it is technically feasible to observe sources in track-sharing with different integration times. This case is not implemented yet in the sensitivity estimator and the different sensitivities should be computed independently. As for single source projects, $\eta_{\rm tel}$ is set to 1.6 in track-sharing mode.

4.3 Mosaicking

Mosaicking is a particular case of wide-field imaging: The user wishes to observe a given field of view larger than the primary beam size with a sensitivity as uniform as possible.

The targeted field (which area is $A_{\rm map}$, define by the user) can be divided in a number of independent resolution elements or independent (primary) beams $n_{\rm beam}$. We have:

$$n_{\rm beam} = \frac{A_{\rm map}}{A_{\rm beam}} \tag{25}$$

where $A_{\rm beam}$is the area of the primary beam. It is linked to the telescope full width at half maximum (θ) by

$$A_{\rm beam} = \frac{0.8\,\pi\,\theta^2_{\rm prim}}{4\,\ln(2)}, \tag{26}$$

The 0.8 factor represents the truncation of the beam at 20% of its maximum, which is performed during the imaging process.

Note that $n_{\rm beam}$ is not the number of pointed positions that are observed for the mosaic ($n_{\rm point} > n_{\rm beam}$, see below).

For the sensitivity estimation we assume a standard sampling of targeted field and the on-source time is equally divided between the independent primary beams $n_{\rm beam}$ in the targeted field of view. To first order, we thus yield:

$$\sigma_{\rm Jy} = \frac{J^{\rm int}_{\rm ant}\,T_{\rm sys}}{\eta_{\rm spec}\,\sqrt{n_{\rm ant}\,(n_{\rm ant}-1)\,d\nu\,n_{\rm pol}\,\Delta t_{\rm on}}} \tag{27}$$

$$\text{with} \quad \Delta t_{\rm on} = \frac{\Delta t_{\rm tel} \,-\, n_{\rm track} \times \Delta t_{\rm tune}}{\eta_{\rm tel} \times n_{\rm beam}} \tag{28}$$

There are several subtleties in this computation.

- $A_{\rm map}$ must be larger than 2 times $A_{\rm beam}$ (below this we advise to use the track sharing mode with two independent fields).

- The processing (imaging and deconvolution) of a mosaic implies a division by the primary beam of the interferometer. As the primary beam is to first order a Gaussian decreasing to zero, this implies that the noise of the mosaic will vary over the field of view. In particular it increases sharply at the edges of the field of view. In other words, Eq. 27 does not apply to the mosaic edges!

- The cycling of the pointings of the mosaic should ensure Nyquist sampling of the observed field of view. This implies that there is an important redundancy between the pointings, contrary to track sharing where the sources are supposed to be fully independent on the sky. For instance, when mosaicking with a hexagonal compact pattern, each line of sight will be observed by 7 contiguous pointings, except at the mosaic edges. It can thus been shown that the number of mosaic pointings, $n_{\rm point}$, is related to the number of independent elements through

$$n_{\rm point} = n_{\rm beam}\,\left(\frac{7}{4}\right)^2, \tag{29}$$

  for a correctly sampled mosaic. Equation 27 is only valid inside a correctly sampled mosaic.

- The pointings of a mosaic must be observed in short time cycles to ensure that all pointings are observed with similar weather conditions and that they share similar *uv* coverage. This minimizes the shift-variant part of the interferometer wide-field imaging response. This calls for the shortest possible integration time per pointing. However, the interferometer takes time to slew from one pointing to the next one without integrating. As a result, the observing efficiency $\eta_{\rm tel}$ is degraded in the cases of mosaics and we have another relationship between the elapsed telescope time and the on-source time as:

$$\Delta t_{\rm on} = \frac{\Delta t_{\rm tel} \,-\, n_{\rm tracks} \times \Delta t_{\rm tune}}{\eta_{\rm tel}\eta_{\rm mos} \times n_{\rm beam}} \quad \text{with} \quad \eta_{\rm mos} = \frac{\Delta t + \Delta t_{\rm slew}}{\Delta t}, \tag{30}$$

where Δt is the integration time per pointing and $\Delta t_{\rm slew}$ is the time to slew between two consecutive pointings. Having a large integration time per pointing compared to $\Delta t_{\rm slew}$ will decrease the mosaicking overhead. This requirement is in sharp contrast with the previous one, namely the need to homogenize the interferometer wide-field response. The best compromise comes from two different considerations.

1. The smallest integration time is set by the acquisition system (for instance, the maximum achievable data rate). In pratice, we enforce that

$$\Delta t_{\rm min} = 10\,{\rm sec}. \tag{31}$$

2. The distance covered by a visibility in the uv-plane during an integration should always smaller than the distance associated to tolerable aliasing (see Pety and Rodríguez-Fernández 2010 for more details). This can be written as the following condition (Eq. C.3 in this article)

$$\frac{\Delta t}{1s} << \frac{6900}{\theta_{\rm alias}/\theta_{\rm syn}}, \tag{32}$$

where $\theta_{\rm alias}$ is the map angular size, and $\theta_{\rm syn}$ the angular resolution. For a given angular resolution, the interferometer minimum integration time corresponds to

$$\Delta t_{\rm min} \leq \frac{1}{\eta}\,\frac{6\,900}{1\,{\rm sec}}\,\sqrt{\frac{\theta_{\rm maj}\theta_{\rm min}}{A_{\rm map}}}, \tag{33}$$

where η is a ad-hoc integer set to 5 to ensure the condition defined in Eq. 32.

As the typical slew time between two pointings is $\Delta t_{\rm slew} = 11\,{\rm sec}$, we yield that

$$1 \leq \eta_{\rm mos} \leq 2.3 \tag{34}$$

- If the time to cycle all the pointings, $\Delta t_{\rm cycle}$, is set to 45 minutes, we yield that the maximum number of pointing per track is

$$n^{\rm max}_{\rm point/track} = \frac{\Delta t_{\rm cycle}}{\Delta t_{\rm min} + \Delta t_{\rm slew}} = 130. \tag{35}$$

- Finally, if the PI wishes to observe an area that will require more that 130 pointings per independent track, the estimator will ask to either increase the requested elapsed telescope time or to decrease the requested field-of-view area. The computation is done as follows.

1. The number of tracks is then computed as described in section 4.1.
2. The number of point per track is then $n_{\rm point/track} = \left(\frac{7}{4}\right)^2 \frac{n_{\rm beam}}{n_{\rm track}}$. This value must be lower than $n^{\rm max}_{\rm point/track}$.

In summary, the sensitivity of a Nyquist sampled mosaic is

$$\sigma_{\rm Jy} = \frac{J^{\rm int}_{\rm ant}\,T_{\rm sys}}{\eta_{\rm spec}\,\sqrt{n_{\rm ant}\,(n_{\rm ant}-1)\,d\nu\,n_{\rm pol}\,\Delta t_{\rm on}}} \tag{36}$$

$$\text{with} \quad \Delta t_{\rm on} = \frac{\Delta t_{\rm tel} \;-\; n_{\rm tracks} \times \Delta t_{\rm tune}}{\eta_{\rm tel}\eta_{\rm mos}n_{\rm beam}} \tag{37}$$

4.4 Dual band observations

In order to observe two frequencies simultaneously, the beam has to be split into two beams with the help of a dichroic. This adds some instrumental noise that we will encode as a higher value of the receiver noise (i.e., in increasing $T_{\rm rec}$ by for instance 10 K).

As the dichroic can be removed from the optical path when doing single band observations, this $T_{\rm rec}$ increases will only happen when the sensitivity estimation is done in dual band mode.

4.4.1 Python implementation

- Session parameters:
  - `tsys_table_line_dbr = ?` path to DBR specific Tsys table (line); may not be defined if not needed by user inputs,
  - `tsys_table_cont_dbr = ?` path to DBR specific Tsys table (continuum); may not be defined if not needed by user inputs.
- User inputs:
  - `dbr_mode = True|False` (False if not defined).

4.5 Frequency cycling observations

In frequency cycling, the tuning frequency is regularly cycled between $n_{\rm freq}$ predefined values inside the same receiver RF band. This first imply that the on-source observing time must be split between the different tuning of the frequency cycling. To do this, the user will have to give the percentage of the time required per tuning. The sum of the percentage will have to be equal to 100%. By default, PMS will divide equally the on-source time between the tunings, and the user will have the possibility to modify this time repartition.

Frequency cycling also has two consequences on the observational efficiency.

1. The time to setup the tunings is increased with respect to standard observations by $(n_{\rm freq}-1)*\Delta t_{\rm freq}$, where $\Delta t_{\rm freq}$ is typically XXX minutes.
2. After the setup phase, each cycle observed at a given frequency must be surrounded by gain calibration observations at the same frequency. This means that the observing efficiency is decreased: in practice this is like doubling the number of calibrators, since each calibrator will have to be observed at the 2 frequencies (the frequencies of the previous and of the next cycle, whatever the number of cycles).

   To take this into account, we first define the overhead factor as

$$\Omega = \frac{1}{\eta_{\rm tel}}. \tag{38}$$

   The overheads are now split into generic overheads, independent of the number of gain calibrators, and the calibration overheads that is directly proportional to the number of observed gain calibrators. This gives

$$\Omega = \Omega_{\rm gen} + n_{\rm gaincal}\,\Omega_{\rm gaincal}\,\Omega_{\rm cycling}. \tag{39}$$

   We will use $\Omega_{\rm gen} = 1.3$ and $\Omega_{\rm gaincal} = 0.3$, $n^{\rm def}_{\rm gaincal} = 1$ or 2 for detection or imaging, respectively, and $\Omega_{\rm cycling} = 2$ in frequency cycling mode, 1 otherwise.

3. The overall overheads are evaluated by computing the total on-source time over the total telescope time:

$$\Omega_{\rm total} = 1 - \frac{\Delta t_{\rm on}}{\Delta t_{\rm tel}} \tag{40}$$

In the context of frequency cycling, the overheads for a single frequency are computed by weighting the times with the fraction r_f spent on this cycle (*e.g.* 50% for 1 among 2 frequencies):

$$\Omega_{\rm total} = 1 - \frac{\Delta t_{\rm on} \times r_f}{\Delta t_{\rm tel} \times r_f} \tag{41}$$

which is identical to the previous formula. If the overheads reach 75%, a warning is raised.

When frequency cycling is combined with dual band observations, it is emphasized that both receiver bands are affected by the efficiency loss of the frequency cycling even though one of the two bands could not require frequency cycling at all.

4.5.1 Python implementation

1. Tuning overheads:
   - Session parameters:
     - `ttune = 40 min` is renamed `ttune_main` (already a mandatory parameter),
     - `ttune_per_freq_cycle = xxx min` (0 if not defined).
   - User inputs:
     - `cycle_nfreq = 1 or more` (1 if not defined, if 1: not a frequency cycling estimation).
2. Observing efficiency:
   - Session parameters:
     - `obseffref = 1.6` already defined is ignored if next parameters are defined,
     - `obseffgen = 1.3`,
     - `obseffgaincal = 0.3`,
     - `ngaincal_detection = 1`,
     - `ngaincal_imaging = 2`,
     - `ngain_cycling = 2`.
   - User inputs:
     - `target_kind = code_detection|code_imaging` (detection if not defined *i.e.* same as before),
     - `cycle_time_frac = 0 to 1` (1 if not defined; if 1: not a frequency cycling estimation).

References

Kraus, J. D., in McGraw-Hill 1982 (1966), Radio Astronomy.